

Kinetic and thermodynamic studies of Co(II), Ni(II) and Mn(II) adsorption using ResinexTM K-8H resin.

M.A. Wassel, A.A. Swelam, A.M.A. Salem, A.S. El-Feky

Department of chemistry, Faculty of Science, Al-Azhar university, Cairo, Egypt

ABSTRACT

Kinetic and thermodynamic studies have been carried out on the adsorption of Co(II), Ni(II) and Mn(II) by strong cation exchange of ResinexTMK-8H (H⁺-form) resin. The adsorption process has been investigated as a function of adsorbate concentration, solution acidity, contact time, adsorbent amount, and temperature. The experiments were performed in batch mode, where the initial concentration on the solution samples were 0.001, 0.0025, 0.005 and 0.01 (mg/l), HCl acid concentration range was 0.01–1.5 (mg/l) and sorbent amount were 0.25, 0.5, 1.5 and 3.0 g. Equilibrium isotherm data were analyzed using Langmuir, Freundlich, and Temkin isotherm models. The results showed that the adsorption process was well described by Freundlich and Langmuir isotherm models. The kinetic data were analyzed using first-order and pseudo-second order kinetic models. The results indicated that adsorption fitted well with the first-order for Mn(II) and pseudo-second order kinetic model for Co(II) and Ni(II). The activation energy, E_a was determined by plotting $\log K_D$ versus $1/T$, as well as the thermodynamic parameters (ΔH , ΔS and ΔG) were determined at different temperatures (25, 35 and 45°C). The values of Co(II) and Ni(II) show endothermic while for Mn(II) show exothermic process. In this study, ion exchange kinetic mechanism for heavy toxic metal ions, Co(II), Ni(II) and Mn(II) is carried out by Strong cation exchange of ResinexTMK-8H (H⁺-form) resin under different conditions in aqueous solution to validate the practical application of this strong cation exchange of ResinexTMK-8H (H⁺-form) resin in wastewater treatment process.

Key words: Thermodynamic, Kinetic, Temperature, ResinexTM K-8H, Adsorption.

Introduction

Divalent metals contamination exists in the aqueous waste streams of many industries, such as metal plating facilities, mining operations, nuclear power plant and tanneries. The soils surrounding many military bases are also contaminated and pose a risk of ground water and surface water contamination due to the divalent metals.

Divalent metals are Cd(II), Cr(III), Co(II), Pb(II) and Hg(II) not biodegradable and tend to accumulate in living organisms, causing various diseases and disorders (Susan *et al.*, 1999, Netzer and Hughes, 1984, Gomez-Lahoz *et al.*, 1993). Cobalt, a natural element present in certain ores of the Earth's crust, is essential to life in trace amounts. It exists in the form of various salts. Pure cobalt is odorless, steely-gray, shiny, hard metal. Everyone is exposed to low levels of cobalt in air, water and food. An average of 2 g in drinking water has been estimated. Cobalt has both beneficial and harmful effect on health. The permissible limits of cobalt in the irrigation water and livestock watering are 0.05 and 1.0 mg dm⁻³, respectively (Wang *et al.*, 2008).

With a better awareness of the problems associated with cobalt, research studies related to the methods of removing cobalt from wastewater have drawn attention increasingly. Cu(II) and Ni(II) are mainly employed in electroplating, pesticides, herbicides and tannery industries. The effluents of these industries usually contain Cu(II) and Ni(II) which can cause environment problems and serious toxicological concerns (Wang *et al.*, 2008).

The current technologies to remove Cu(II) and Ni(II) from water/wastewater include chemical precipitation, adsorption and membrane process. Among these technologies, adsorption is the most common approach for removing divalent metal ions from water/wastewater with high efficiency and easy operation. Many solid materials as adsorbents have been investigated, such as activated carbons (AC), polymeric resins and natural bio-adsorbents (NBA). Comparing with AC and NBA, polymeric resins have been used more widely in the removal of divalent metals from water (Niu *et al.*, 2010, Tugba *et al.*, 2010).

The synthesis and characterization of control ledpore silica modified with N-propylsalicylaldimine has been performed (Abou-El-Sherbini *et al.*, 2002). B/Si ratio of 6.5/1 in borosilicate glass was found effective in obtaining highly porous silica by acid leaching which led to high exchange capacity (CIE11=0.36 mmole Cu g⁻¹, pH 5.5) in the obtained ion exchanger (IE11). The complexation behavior of IE11 with Mn(II), Co(II), Ni(II), Cu(II), Hg(II), Cr(III), Fe(III) and UO₂(II) was investigated and confirmed by electronic and infrared spectra and thermal analysis. Adsorption of Mn(II) on Turkish kaolinite required 120 min to reach equilibrium (Yavuz *et al.*, 2003).

In the solution temperature range of 298 to 313 K, the first order rate coefficient increased from 1.20×10^{-3} to $1.90 \times 10^{-3} \text{ min}^{-1}$ (experimental conditions: adsorbent 1.0 g and particle size 200 mesh).

Materials And Methods

- *Materials*

All the materials and chemicals (Aldrich, USA) were used as received with analytical grade. Stock solutions of Co(II), Mn(II) and Ni(II) were prepared by dissolving its chloride (AR Grade) in distilled water. The stock solution was diluted with distilled water to obtain the desired concentrations. Strong cation exchange of Resinex™K-8H (H⁺-form) used in this work from Jacobi Swedish Company. Prior to use, the resin was converted to the hydrogen (H⁺) form by washing it in 1 M HCl followed by further washing in deionised water. The resin regeneration procedures follow the recommendations provided by the manufacturers. The resin-H was dried and kept at room temperature in a desiccators until it was used.

The adsorption capacity in mg/g of the adsorbent (q_e) and the metal ion adsorption percentage (Ad%) were obtained by Eqs. (1) and (2),

$$q_e = \frac{(C_0 - C_e)V/1000}{W} \quad (1)$$

$$\text{Ads\%} = \frac{(C_0 - C_e) \times 100}{C_0} \quad (2)$$

where C_0 and C_e are the initial and final metal ion concentrations (mg/l), respectively, V is aqueous phase volume (ml) and W is the weight of adsorbent used (g). The data of isotherms were obtained after an equilibrium time of 24 h. After the equilibrium time, the concentrations were determined by AAS varion 6 (Analytik Jena AG Konrad-Zuse-StraBe 1 07745 Jena).

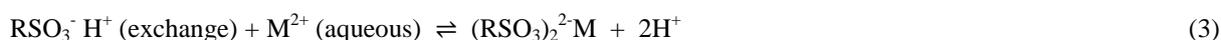
- *Batch adsorption studies:*

Adsorption studies were carried out in a batch mode by shaking 0.5 g resin in 50 mL solution of Co(II), Ni(II) and Mn(II) with concentration range from 158 to 675 mg/l on the water bath shaker at 100 rpm stirring speed. Effect of solution acidity on the Co(II), Ni(II) and Mn(II) adsorption onto Resinex™K-8H was conducted through varying the acidity of HCl solution in the range 0.01–3.0 M. Furthermore the adsorption studies were also carried out by varying time interval (5–210 min) at 452 mg/l of Co(II), Ni(II) and Mn(II) to optimize the time required for the removal of Co(II), Ni(II) and Mn(II) from aqueous solution.

Discussion:

- *Effect of solution acidity:*

Hydrochloric acid was used as complexing agent in a wide range of concentrations namely, 0.01 to 3.0 M. Because the influence of this acid, hydrogen ion is governed by the mass reaction equation for a simple exchange action of the chloride ion by lowering the effective concentration of the cation in solution through complex formation. In order to investigate the effect of acidity solution on the metal ions uptake on Resinex™K-8H strong acid cation exchange resin, series of experiments were carried out at 25°C using 0.50 g Resinex™K-8H, and at a constant concentration, 452 mg/L of M^{+2} ($M^{+2} = \text{Ni(II), Co(II) and Mn(II)}$) in aqueous solution with alter initial acidity values from 0.1 to 3.0M. The equilibrium uptake, q_e (mg/g) of Ni(II), Co(II) and Mn(II) on Resinex™K-8H from different acidic media was carried out. The effect of HCl at acid concentration ranging from 0.01 to 1.5 M on the uptake of these metal ions are presented in Fig. 1. The equilibrium sorption data indicate that: (i) At low acid concentration the metal cations exhibit generally strong uptake and high affinity with the Resinex™K-8H matrix. This behavior is a prominent for all sorption processes. However, (ii) With increasing acid concentration the H⁺ increase and further competes the exchange sites. This behavior indicates that the ion exchange equilibrium shown in Eq.3:



is predominant in back direction with the increase in acid concentration. (iii) Within the studied acid concentrations range, in general, the sorption of cations in majority follows the selectivity order; Co(II) > Ni(II) > Mn(II). This may be explained in terms of the stability constants of the complexes which the metal ions form with these acids. This acid might form rather stronger complexes with Co(II) > Ni(II) > Mn(II). According

to the above reaction (Eq. 3), low acidity will favor forward reactions whereas high acidity will favor backward reactions. Although all these listed adsorption reactions might take place, their extent (completeness) for specific ion species is very different due to the different affinity and selectivity of the resin to positively charged ions, which the base for the adsorption processes.

Fig. 1 shows the uptake of Co(II), Ni(II) and Mn(II) as a function of acidity. It can be seen that the higher of metal ions uptake is maximum at acidity of 0.01M. At higher than 1.0M the uptake decreases continuously until it vanishes (0%) at 3.0 M for each these metal ions.

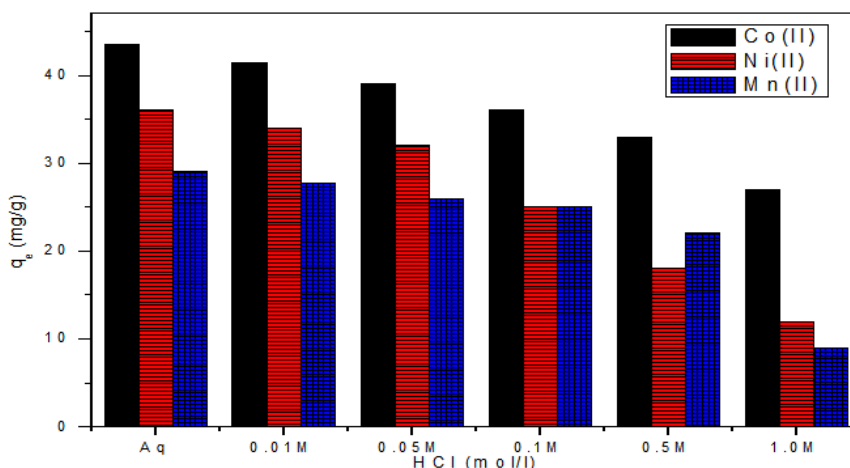


Fig. 1: Effect of HCl concentrations for the adsorption uptake of Co (II), Ni (II) and Mn (II). At 25 °C.

The first stage of ion exchange is deprotonation of the sulphonic group of Resinex™K-8H which is represented by Eq. 3. The zero percent removal at 3.0 M can be attributed to the fact that at higher acidity, the concentration of H^+ in the adsorption medium shifts the equilibrium as shown in Eq. 3 to the left direction. This means that the sulphonic groups of the cation exchange resin do not ionize and the ion exchange sites on the cation exchange resin surface are still protonated, under such conditions the metal ions do not exchange and remain in the solution. As the acidity decreases from 3.0 to 0.01 M, the deprotonation equilibrium is shifted to right and as a result, the adsorption capacity increases until it reaches its maximum values at 0.01 M (Mouni *et al*, 2011).

- *Effect of adsorbent dosage:*

The effect of adsorbent dosage on the percentage removal of Co(II), Ni(II) and Mn(II) by Resinex™ K-8H strong acid cation exchange resin are depicted in Fig.2, it can be seen that for Co(II) and Ni(II), as the dosage increased from 0.25 to 1.5 g at 25°C, the adsorption capacity of metal ions at equilibrium, q_e , shows increases. Additionally, higher adsorbent dosage, i.e., more than 1.5 g, complete sorption occur, while Mn(II) show complete sorption after 3.0 g of the Resinex™ K-8H (Sari *et al*, 2007, Azouaou *et al*, 2010, Iqbal *et al*, 2009) indicating that a larger quantity of readily active sites are available for adsorption.

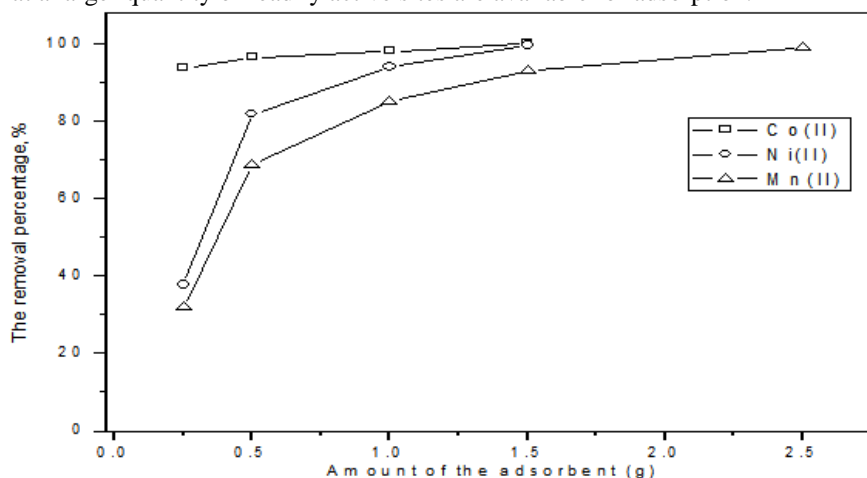


Fig. 2: Effect of amount of the Resinex™ K-8H on the removal percentage of Co (II), Ni (II) and Mn (II). at 25 °C.

- *Effect of contact time and adsorption kinetics:*

The obtained data for the Co(II), Ni(II) and Mn(II) removal from aqueous solution using the Resinex™K-8H is presented in (Fig. 3). The adsorption of Co(II), Ni(II) and Mn(II) from aqueous solution onto the Resinex™K-8H was rapid at the start of experiment and then rate of adsorption become slow down. The maximum amount of Co(II), Ni(II) and Mn(II) from aqueous solutions was adsorbed onto the Resinex™K-8H within 150 min for Co(II), Ni(II) and 210 min for Mn(II) respectively, then no significant change was observed. Thus the time of equilibrium for the Co(II), Ni(II) was 150 min and 210 min for Mn(II) respectively, then no significant change was observed. Thus the time of equilibrium for the Co(II), Ni(II) was 150 min and 210 min for Mn(II) adsorption onto the Resinex™K-8H ion-exchange resin from aqueous solutions. The probable reason for rapid adsorption of Co(II), Ni(II) and Mn(II) onto the Resinex™K-8H from aqueous solution may be more available active sites in the Resinex™K-8H for adsorption. In addition the $-SO_3H$ and groups in the Resinex™K-8H were responsible for the complex formation between metal ions Co(II), Ni(II) and Mn(II) and functional groups ($-SO_3H$) (Dam and Kim, 2009, Vellaichamy and Palanivelu, 2011). However the more active sites may not be available in the Resinex™K-8H for further metal ions adsorption with progress of contact time.

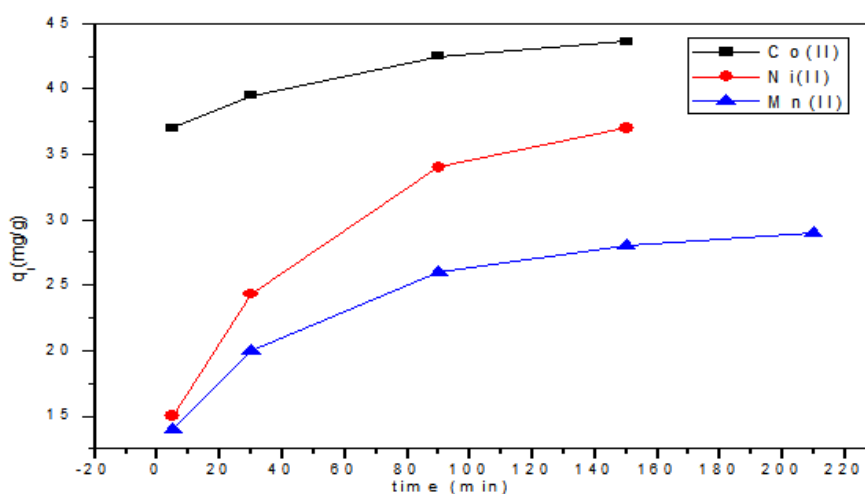


Fig. 3: Effect of contact time on the adsorption uptake of Co (II), Ni (II) and Mn (II). at 25 °C.

The pseudo-first-order and pseudo-second-order also intraparticle diffusion kinetic models were applied to determine the adsorption rate of Co(II), Ni(II) and Mn(II) onto the Resinex™K-8H. The linear equation for pseudo-first-order kinetic model can be expressed as:

$$\log(q_e - q_t) = \log q_{e,1} - k_1 t \quad (4)$$

Lagergren showed that the rate of adsorption of solute on the adsorbent is based on the adsorption capacity and followed a pseudo-first-order equation (Lagergren *et al*, 1898, Yang and Al-Duri, 2005) which is often used for estimating k_1 considered as mass transfer coefficient in the design calculations. where q_e and q_t are the amounts of the metal ion adsorbed (mg/g) at equilibrium time and at any instant of time t , respectively, and k_1 (L/min) is the rate constant of the pseudo-first-order adsorption. The plot of $\log(q_e - q_t)$ versus t gives a straight line (Fig.4) for the pseudo first-order adsorption kinetics, from the adsorption rate constant, k_1 , is estimated.

Ho developed a pseudo second-order kinetic expression for the adsorption system of divalent metal ions. This model has since been widely applied to a number of metal/sorbent adsorption systems. The adsorption of Co(II), Ni(II) and Mn(II) onto the Resinex™K-8H resin at a short time scale may involve a chemical sorption which implies the strong electrostatic interaction between the Resinex™K-8H functional groups surface and each of Co(II), Ni(II) and Mn(II). The linear equation for pseudo-second-order kinetic model can be expressed as (McKay and Ho, 1999). The second-order kinetics equation is described as in the following form:

$$\frac{t}{q_t} = \frac{1}{k_2 q_e^2} + \frac{t}{q_e} \quad (5)$$

where k_2 (g/mg min) is the second-order rate constant. The product $k_2 q_e^2$ is the initial adsorption rate "h" (mg/g min):

$$h = k_2 q_e^2 \quad (6)$$

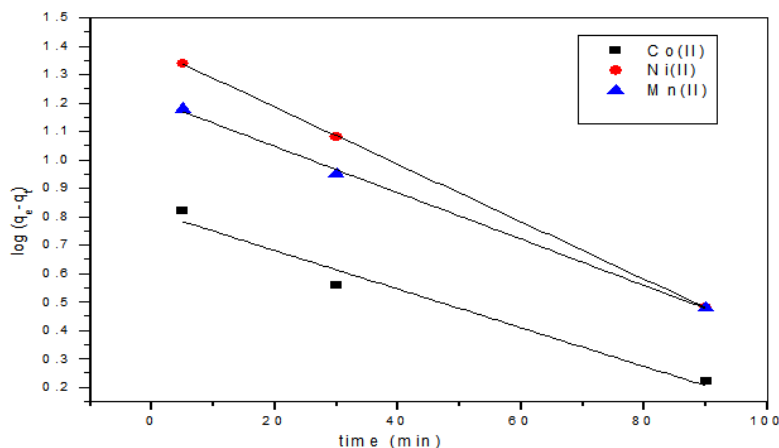


Fig. 4: Pseudo-first order kinetic plots for the adsorption uptake uptake of Co (II), Ni (II) and Mn (II) at different temperatures

Which h can be regarded as the initial adsorption rate as t approaches 0. Under such circumstances, the plot of t/q_t versus t should give a linear relationship as in (Fig.5), which allows the computation of q_e and k_2 . Where k_2 is the pseudo-second-order rate constant ($\text{g mg}^{-1} \text{min}^{-1}$). The q_{e1} , q_{e2} , k_1 and k_2 values for different temperatures of Co(II), Ni(II) and Mn(II) solutions were calculated from their respected plots.

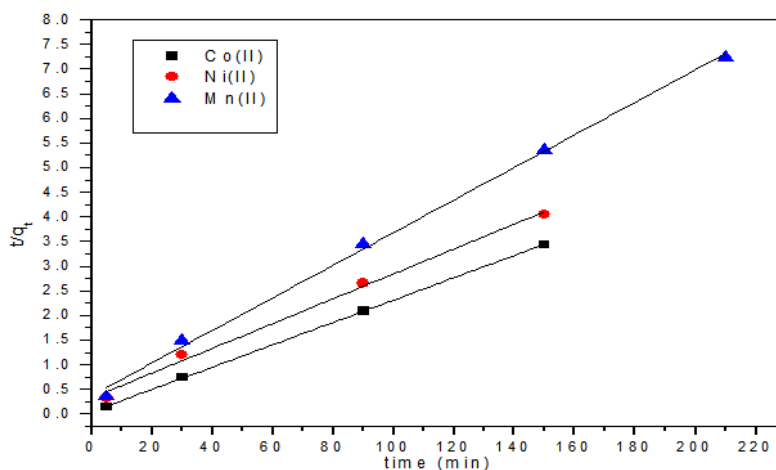


Fig. 5: Pseudo- second kinetic plots for the adsorption uptake uptake of Co (II), Ni (II) and Mn (II) at different temperatures

The obtained q_{e1} , q_{e2} , k_1 , k_2 and correlation coefficient (R^2) values are tabulated in Table 1. The R^2 values of Co(II) for pseudo second-order kinetic model are relatively higher than pseudo-first order kinetic model adsorption. However, the experimental q_e values are very close to the calculated q_{e2} values for pseudo-second-order kinetic model.

These results implied that the adsorption of Co(II), onto the ResinexTMK-8H obeyed second order kinetic model (McKay and Ho, 1999, Chen and Li, 2010), while opposite trend was observed for the Ni(II) and Mn(II), where the R^2 values for pseudo first-order kinetic model are relatively higher than pseudo-second order kinetic model adsorption. These results implied that the adsorption of Ni(II) and Mn(II), onto the ResinexTMK-8H obeyed first-order kinetic model. The diffusion of metal ions cannot be explained on the basis of pseudo-first-order and pseudo-second-order kinetic model.

Due to this reason, intraparticle diffusion model was applied to estimate the diffusion of Co(II), Ni(II) and Mn(II) in the ResinexTMK-8H using Weber–Morris intraparticle diffusion model (Weber *et al.* 1963):

$$q_t = k_p t^{1/2} + C \quad (7)$$

where k_p is the intraparticle diffusion rate coefficient ($\text{g mg}^{-1} \text{min}^{1/2}$) and C provides an idea about the thickness of the boundary layer. The plot of q_t vs. $t^{1/2}$ as in (Fig.6) shows the three straight-line portions with three different slopes and intercept values. First portion of curves indicates the boundary layer diffusion while

final linear portion is a result of the intra-particle diffusion. Boundary layer is dominant if the intercept values are high as in Ref. (Oubagaranadin *et al*, 2007).

Table 1: Kinetic parameters for of Ni(II), Co(II) and Mn(II) on Resinex™ K-8H in aqueous solution.

	Pseudo first-order model			Pseudo second-order model			Intraparticle diffusion model			
	$q_{e,1,cal}$	K_1	$R^2 q_{e,2,cal}$	K_2	h	R^2	K_{int}	C	R^2	
	(mg/g)	(min^{-1})		(mg/g)	(g/mg min)	(mg/g min)	($\text{mg/g min}^{-0.5}$)	(mg/g)		
Ni(II)										
Temp.K										
298	24.40	0.0220	0.9998	39.70	1.5×10^{-3}	2.36	0.9907	2.21	11.43	0.9551
308	28.64	0.0222	1.0000	45.50	1.7×10^{-3}	3.52	0.9936	2.63	11.38	0.9694
318	29.43	0.0230	0.9970	47.00	1.9×10^{-3}	4.20	0.9936	2.60	13.87	0.9574
Co(II)										
298	7.56	0.0290	0.9955	44.09	12.0×10^{-3}	23.30	0.9997	0.68	35.92	0.9387
308	7.99	0.0356	0.9963	44.70	13.0×10^{-3}	25.98	0.9998	0.65	37.03	0.9126
318	8.45	0.0366	0.9846	45.45	15.0×10^{-3}	30.99	0.9999	0.61	38.25	0.8898
Mn(II)										
298	17.26	0.0286	0.9993	30.27	2.9×10^{-3}	2.66	0.9971	1.24	12.51	0.9379
308	16.76	0.0161	0.9904	28.43	2.2×10^{-3}	1.87	0.9916	1.25	9.85	0.9806
318	16.20	0.0141	0.9984	26.84	1.7×10^{-3}	1.22	0.9853	1.32	6.42	0.9876

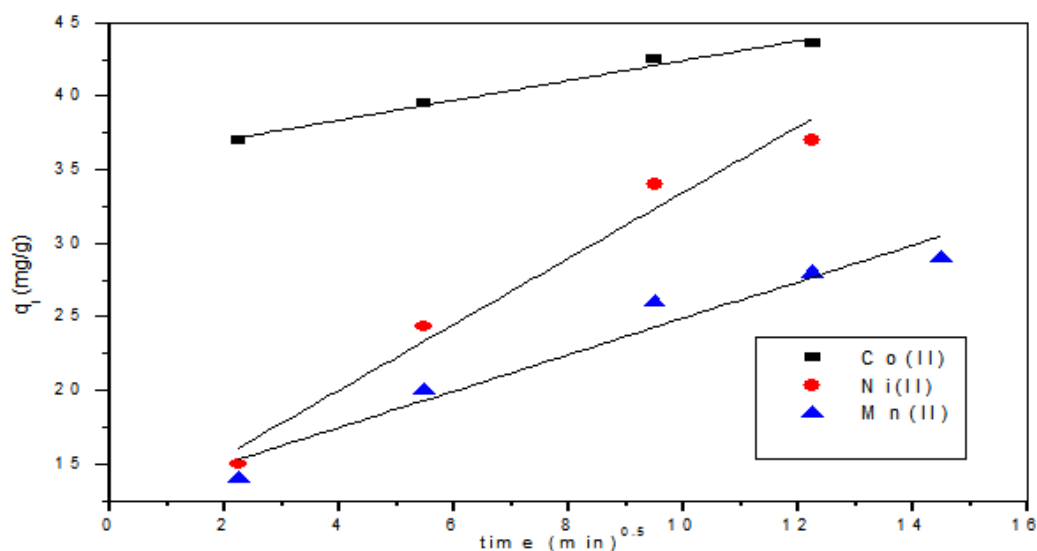


Fig. 6: Plots of Weber-Morris for the adsorption of uptake of Co (II), Ni (II) and Mn (II) at 25 °C

The intercept values for Ni(II), Co(II) and for Mn(II) is 11.43, 35.92 and 12.51 mg g^{-1} respectively. The obtained values indicated that adsorption of Co(II), Ni(II) and Mn(II) onto the Resinex™ K-8H was controlled through a boundary layer effect.

- *Effect of concentration and adsorption isotherm:*

The adsorption of Co(II), Ni(II) and Mn(II) onto the Resinex™ K-8H at 25°C and different concentrations is depicted in Fig. 7. It was observed that the adsorption of Co(II), Ni(II) and Mn(II) onto the Resinex™ K-8H increased with rise in concentration of these metal ions from 158 to 675 mg L^{-1} . This is attributed to the greater driving force through a higher concentration gradient at high metal ions concentration according to (Acemioglu, 2005, Hameed *et al*, 2008, Ramkumara and Mukherjee, 2007). Thus the developed Resinex™ K-8H can be efficiently used for the removal of high concentration Co(II), Ni(II) and Mn(II) from aqueous solutions. The surface property and affinity of Resinex™ K-8H for Co(II), Ni(II) and Mn(II) removal can be determined using the different adsorption isotherm models.

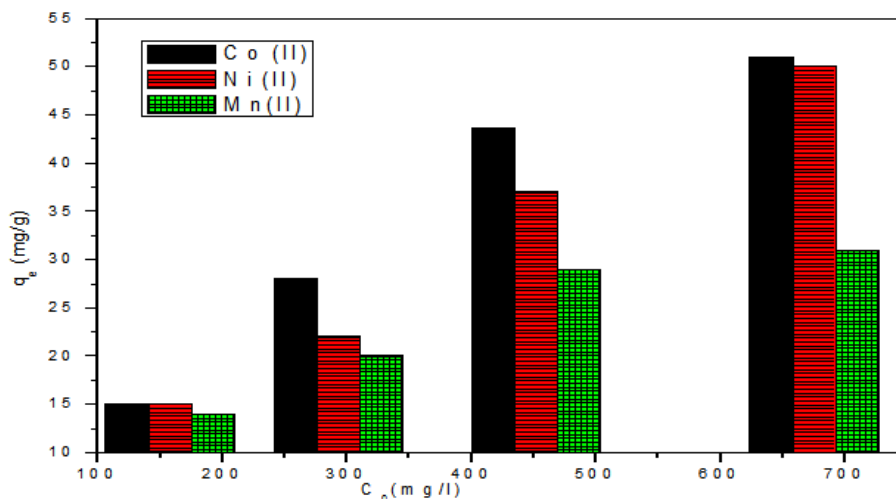


Fig. 7: Effect of initial metal ion concentration on the adsorption uptake of Co (II), Ni (II) and Mn (II). at 25 °C.

The obtained equilibrium data from the adsorption of Co(II), Ni(II) and Mn(II) onto the Resinex™K-8H fitted to the linear equation of Langmuir, Freundlich, and Temkin and Pyzhe isotherm models. The linear equation for Langmuir, Freundlich and Temkin isotherm models are expressed as follows:

The model takes the following linear form:

$$\frac{C_e}{q_e} = \frac{1}{bQ_0} + \frac{C_e}{Q_0} \quad (8)$$

where Q_0 is the quantity of adsorbate required to form a single monolayer on unit mass of adsorbent (mg/g) and q_e is the amount adsorbed on unit mass of the adsorbent (mg/g) when the equilibrium concentration is C_e (mg/l) and b (L/mg) is Langmuir constant that is related to the apparent energy of adsorption. As in Eq.(3) shows that a plot of (C_e/q_e) versus C_e should yield a straight line if the Langmuir equation is obeyed by the adsorption equilibrium.

The slope and the intercept from (Fig.8) of this line yield the values of constants Q_0 and b respectively. A further analysis of the Langmuir equation can be made on the basis of a dimensionless equilibrium parameter, R_L (Altin *et al.*, 1998), also known as the adsorption factor, given by Eq. (9):

$$R_L = \frac{1}{1 + bC_0} \quad (9)$$

The value of R_L lies between zero and one for a favorable adsorption, while $R_L > 1$ represents an unfavorable adsorption, and $R_L = 1$ represents the linear adsorption, while the adsorption operation is irreversible if $R_L = 0$.

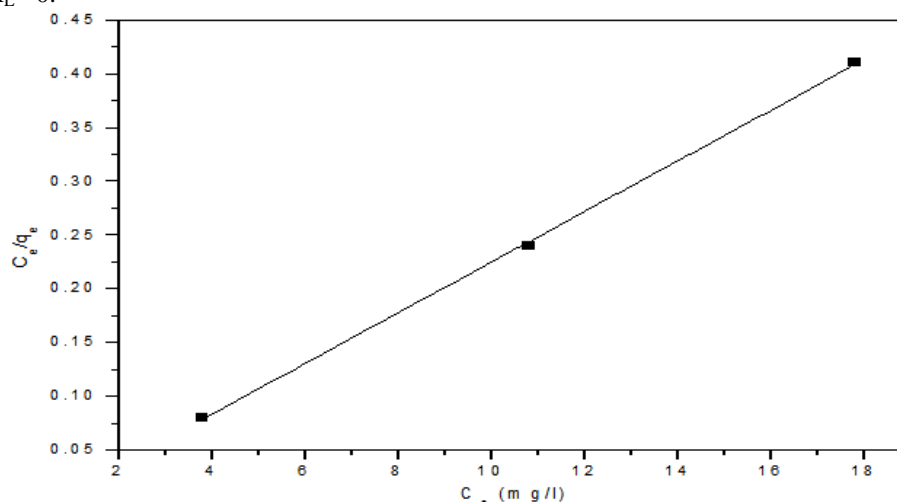


Fig. 8: Langmuir plot for the adsorption of Co (II) at different temperatures.

The Freundlich isotherm theory says that the ratio of the amount of solute adsorbed onto a given mass of sorbent to the concentration of the solute in the solution is not constant at different concentrations. The heat of adsorption decreases in magnitude with increasing the extent of adsorption (Koopal *et al*, 1994). The linear Freundlich isotherm is commonly expressed as follows:

$$\log q_e = \log k_F + (1/n) \log C_e \quad (10)$$

where K_F and n are the Freundlich constants characteristics of the system, indicating the relative adsorption capacity of the adsorbent related to the bonding energy and the adsorption intensity, respectively. A plot of $\ln q_e$ versus $\ln C_e$ as in (Fig.9) yielding a straight line indicates the confirmation of the Freundlich isotherm for adsorption. The constants which are K_F and $1/n$ can be determined from the slope and the intercept respectively according to (Agrawal *et al*, 2004).

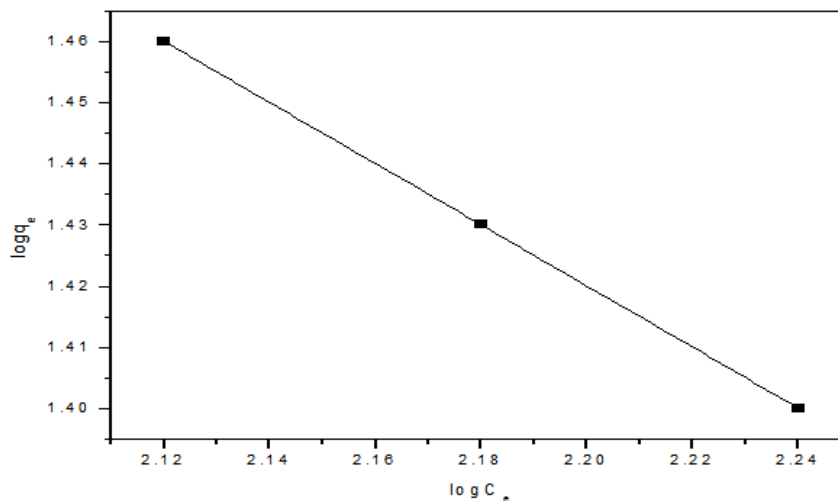


Fig. 9: Freundlich isotherm plot for the adsorption of Mn (II)

Temkin isotherm model assumes that the heat of adsorption of all the molecules in the layer decreases linearly with the coverage of molecules due to the adsorbate–adsorbate repulsions and the adsorption of adsorbate is uniformly distributed and that the fall in the heat of adsorption is linear rather than logarithmic. The linearized Temkin equation is given by Eq. (11):

$$q_e = B_T \ln A_T + B_T \ln C_e \quad (11)$$

where $B_T = RT/b_T$, T is the absolute temperature in K and R is the universal gas constant ($8.314 \text{ J mol}^{-1} \text{ K}^{-1}$). The constant b_T is related to the heat of adsorption, A_T is the equilibrium binding constant (L min^{-1}) corresponding to the maximum binding energy. The slope and the intercept from a plot of q_e versus $\ln C_e$ as in (Fig.10) determine the isotherm constants A_T and b_T .

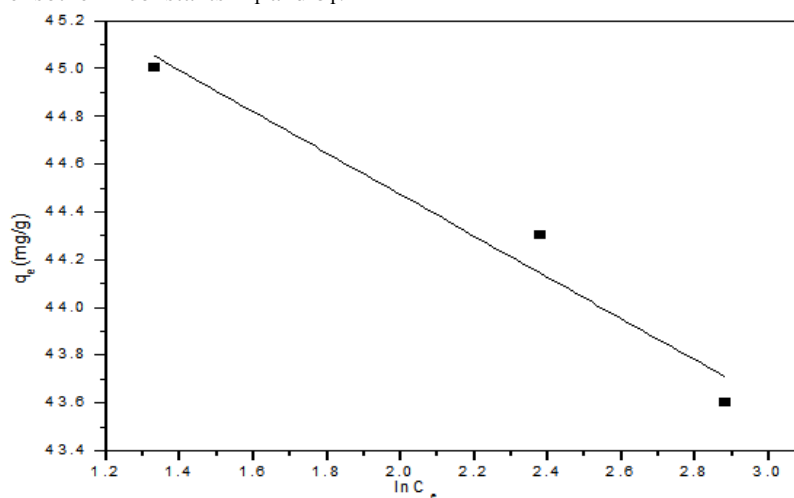


Fig. 10: Temkin plot for the adsorption of Co (II) at different temperatures

The obtained values of applied adsorption isotherm parameters are reported in Table 2. Values of R^2 indicated that Langmuir isotherm model for the Ni(II) and Co(II) adsorption was best fitted in comparison with Freundlich and Temkin isotherm models. The n values were found to be 11.92 for the Mn(II) adsorption onto the Resinex™K-8H from aqueous solution. These values are suggesting that Resinex™K-8H is better adsorbent for the separation and removal of Ni(II) and Co(II) from aqueous solution. The obtained results for the Ni(II) and Co(II) adsorption are similar to the reported adsorbent by (Özbay, 2009, Monier *et al*, 2010). The Mn(II) have opposite trend than Ni(II) and Co(II), where R^2 values indicated that Freundlich isotherm model for the Mn(II) adsorption was best fitted in comparison with Langmuir and Temkin isotherm models. The n values were found to be 2.52 for the Mn(II) adsorption onto the Resinex™K-8H from aqueous solution. The adsorption capacity of adsorption and removal of Co(II), Ni(II) and Mn(II) from aqueous solution or wastewater are tabulated in Table 2.

Table 2: Adsorption isotherm parameters of Ni(II), Co(II) and Mn(II) on Resinex™K-8H in aqueous solution.

Metal ions	Langmuir parameters			Freundlich parameters			Temkin parameters			
	Q _o	b	R _L	R ²	n	K _f	R ²	k _T	B _T	R ²
	(mg/g) (L/mg)				mg/g		L/g	J/mol		
Ni(II)	35.56	0.28	7.9x10 ⁻³	0.9973	11.92	54.43	0.8644	3.97x10 ⁻⁷	3.63	0.8731
Co(II)	43.22	5.28	4.18x10 ⁻⁴	0.9999	49.93	46.25	0.9202	7.1x10 ⁻²⁴	0.87	0.9194
Mn(II)	17.16	0.018	0.15	0.9965	2.00	331.00	1.0000	1.14x10 ⁻³	15.35	0.9890

• *Temperatures and Thermodynamics parameters of Ni(II), Co(II) and Mn(II) adsorption:*

The effect of temperature on the adsorption of Ni(II), Co(II) and Mn(II) from aqueous solution onto the Resinex™K-8H was performed to evaluate the influence of metal ion adsorption capacity. As it can be seen from Fig. 11, that Ni(II) and Co(II) removal tended to increase with the increase of temperatures. Enhancement of the adsorption capacity at higher temperatures may be attributed to the enlargement of pore size and/or activation of the adsorbent surface according to (Jhaa *et al*, 2008). Opposite trend was also observed for Mn(II) adsorption. This may be due to low stability constant of Mn(II) complex with the Resinex™K-8H.

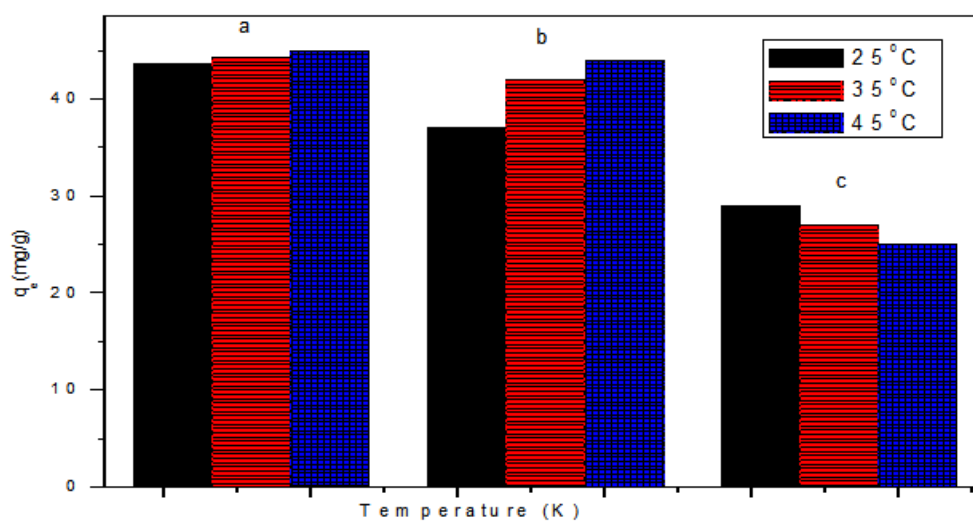


Fig. 11: Effect of temperature on the adsorption uptake of a-Co (II), b-Ni (II) and c-Mn (II).

From Fig. 12, thermodynamic parameters were determined for temperatures ranging from 25 to 45°C using the equilibrium constant K_D (q_e/C_e).

The change in free energy (ΔG°) was determined as follows (Eq. (12)):

$$\Delta G^\circ = -RT \ln K_D \quad (12)$$

where, ΔG° is the standard free energy (kJ/mol), R is the ideal gas constant (8.314 J/mol K). The parameters of enthalpy ΔH° (kJ/mol) and entropy ΔS° (J/mol) related to the adsorption process were calculated by equation (13):

$$\log K_D = \Delta S^\circ/R - \Delta H^\circ/RT \quad (13)$$

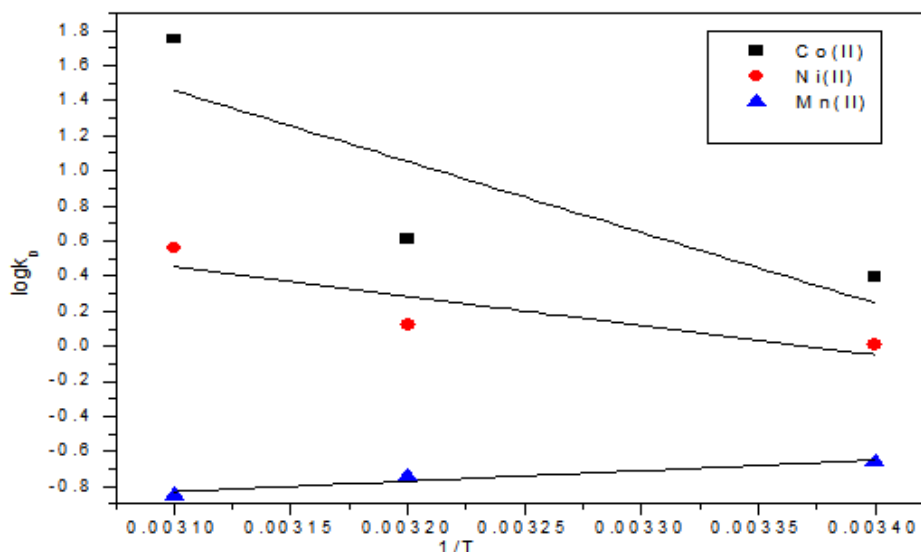


Fig. 12: Van't Hoff plots for the adsorption uptake of Co (II), Ni (II) and Mn (II) at different temperatures

The parameters of enthalpy (ΔH°) and entropy (ΔS°) can be calculated from the slope and the intercept of the linear plot of $\log k_D$ versus $1/T$. The data obtained from the thermodynamic plots and the related parameters are collected in Table 3. The values of ΔH° were positive for Ni(II) and Co(II) indicating that the adsorption process is endothermic in nature. The positive values of ΔS° showed the increased randomness at the solid/solution interface during the adsorption process. The adsorbed water molecules, which were displaced by the adsorbate species, gained more translational energy than was lost by the adsorbate ions, thus allowing the prevalence of the randomness in the system. The negative ΔH° values confirmed the exothermic nature of Mn(II) adsorption. Moreover negative ΔS° value showed reduction in affinity of Mn(II) onto the ResinexTM K-8H. In addition, depending on types of the metal ions. The values of standard free energy change (ΔG°) were negative under the conditions applied, the ion exchange of the metal ions was spontaneous. The values of ΔG° becomes more negative with the increase of temperature for Ni(II) and Co(II) indicated more efficient adsorption at high temperature and hence its adsorption become more favorable. While for Mn(II) values of ΔG° becomes less negative with the increase of temperature indicated lower efficient adsorption at high temperature and hence its adsorption become less favorable at high temperature as in (Arias and Sen, 2009, Samiey and Toosi, 2010, Sepehra *et al.*, 2013, Franco *et al.*, 2013 and Sharma *et al.*, 2013). The result derived from the references and this work indicates that the thermodynamic parameters are related to the nature of metal ions.

Table.3. Thermodynamic parameters for of Ni(II), Co(II) and Mn(II) on ResinexTM K-8H in aqueous solution.

	ΔG (KJ/mol)	ΔS (J/mol k)	ΔH	A (KJ/mol)	Ea (kJ/mol)
Ni(II)					
Temp.K					
298	-0.02	183.85	56.20	3.4×10^{-4}	6.18
308	-0.69				
318	-314				
Co(II)					
298	-2.23	144.40	40.59	12.0×10^{-3}	5.70
308	-10.52				
318	-31.38				
Mn(II)					
298	1.51	-51.51	-11.49	1.15×10^{-5}	13.54
308	1.71				
318	1.97				

The activation energy, E_a (kJ mol^{-1}) can be calculated from Fig.13 using the following equation:

$$\log k_2 = \log A - E_a/RT \quad (14)$$

The positive values of activation energy in Table 3 indicated that the minimum energy is required to facilitate the forward ($M^{2+}-H^+$) ion-exchange process and endothermic process.

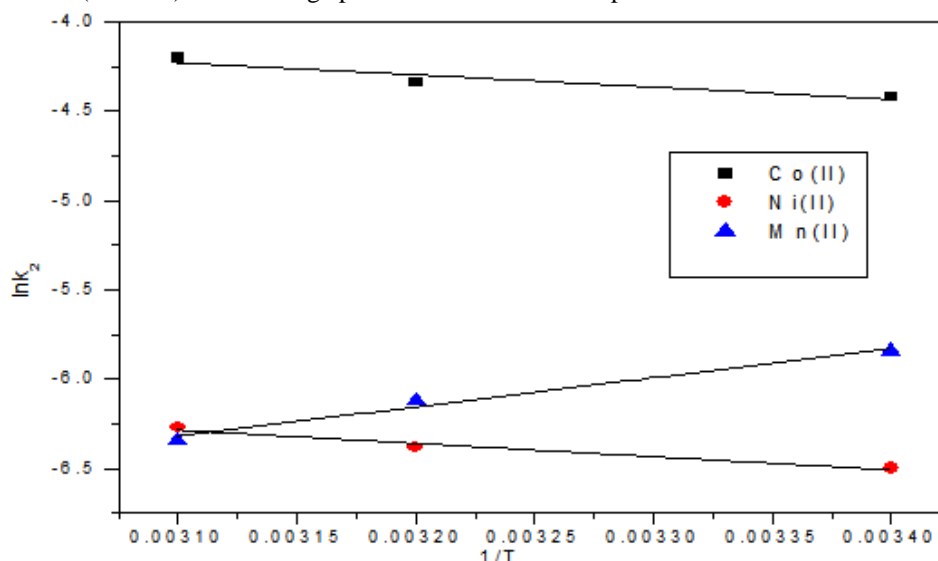


Fig. 13: Arrhenius plots for the adsorption of uptake of Co(II), Ni and Mn(ii)

The order of activation energy to facilitate the ion exchange processes for the divalent metal ions was observed to be $Co(II) > Ni(II) > Mn(II)$. The higher activation energy for Mn(II)-H exchange as compared to Ni(II)-H and Co(II)-H exchange may be considered due to higher ionic radii even though ionic mobility for the metal ions is same (Alothman *et al.*, 2012).

REFERENCES

- Abou-El-Sherbini, Kh., M. Sh. Khalil, U. El-Ayaan, 2002. *JMS&T* 10: 3.
- Acemioglu, B., 2005. *Chem. Eng. J.* 106: 73-81.
- Agrawal, A., K.K. Sahu, B.D. Pandey, 2004. *Colloids Sur. A: Physicochem. Eng. Aspects.*, 237: 133-140.
- Alothman, Z.A., M.M. Alam, M. Naushad, 2012. *J. Indust. Eng. Chem.* in press.
- Altin, O., H.O. Ozbelge, T. Dogu, 1998. *J. Colloid Interf. Sci.*, 198: 130-140.
- Arias, F., T.K. Sen, 2009. *Colloids Surfaces A: Physicochem. Eng. Aspects.*, 348: 100-108.
- Azouaou, N., Z. Sadaoui, A. Djaafri, H. Mokaddem, 2010. *Journal of Hazardous Materials.*, 184: 126-134.
- Chen, Y.H., F.A. Li, 2010. *J. Colloid Interface Sci.*, 347: 277-281.
- Dam, H.A., D. Kim, 2009. *Ind. Eng. Chem. Res.*, 48: 5679-5685.
- Franco, P.E., M.T. Veit, C.E. Borba, G.C. Gonçalves, M.R. Fagundes-Klen, R. Bergamasco, E.A. Silva, P. Y.R. Suzaki, 2013. *Chemical Engineering Journal*, 221: 426-435.
- Gomez-Lahoz, C., F. Garcia-Herruzo, J. Rodriguez-Maroto, J. Rodriguez, 1993. *Water Res.*, 27: 985-92.
- Hameed, B.H., D.K. Mahmoud, A.L. Ahmad, 2008. *Colloids Surface A: Physicochem. Eng. Aspects*, 316: 78-84.
- Iqbal, M., A. Saeed, S. Iqbal Zafar, *J. Hazard. Mater.*, 164: 161-171.
- Jhaa, M.K., R.R. Upadhyay, J.C. Lee, V. Kumar, 2008. *Desalination.*, 228: 97-107.
- Koopal, L.K., W.H. Van Remsdijk, J.C.M. de Wit, M.F., 1994. *J. Colloid Interf. Sci.*, 166: 51-60.
- Lagergren, S., 1898. Zur theorie der sogenannten adsorption gelöster stoffe, *K. Sven. Vetenskapskad. Handl.*, 24: 1-39.
- McKay, G., Y.S. Ho, 1999. *Process Biochem.*, 34: 451-465.
- Monier, M., D.M. Ayad, Y. Wei, A.A. Sarhan, 2010. *J. Hazard. Mater.*, 177: 962-970.
- Mouni, L., D. Merabet, A. Bouzaza, L. Belkhiri, 2011. *Desalination* in press.
- Netzer, A., D. Hughes, 1984. *Water Res.*, 18: 927-33.
- Niu, L., S.B. Deng, G. Yu, *et al.*, 2010. *Chem. Eng. J.* 165: 751.
- Oubagaranadin, J.U.K., N. Sathyamurthy, Z.V.P., *J. Hazard. Mater.*, 142: 165-174.
- Özbay, A., 2009. *Energy Source A* 31: 1271-1279.
- Ramkumara, J., T. Mukherjee, 2007. *Separation and Purif. Technol.*, 54: 61-70.
- Samiey, B., A.R. Toosi, 2010. *Journal of Hazardous Materials.*, 184: 739-745.
- Sari, A., M. Tusen, M. Soylak, *J. Hazard. Mater.*, 144: 41-46.

Sepehri, M.N., M. Zarrabia, H. Kazemianb, A.Amranec, K. Yaghmaian, H.R. Ghaffarie, 2013. *Applied Surface Science*, in press.

Sharma, P., M. Sharma, R. Tomar, 2013. *Journal of the Taiwan Institute of Chemical Engineers* in press in press.

Susan, B., J. Trudy, B. Mark, A. Dean, 1999. *Water Res.*, 33: 2469-79.

Tugba, S.K., K. Esengul, P.O. Sabriye, *et al.*, 2010. *React. Funct. Polym.*, 70: 900.

Vellaichamy, S., K. Palanivelu, J. Hazard, 2011. *Mater.*, 185: 1131-1139.

Wang, H., X.J. Wang, J.F. Zhao, *et al.*, 2008. *Chin. Chem. Lett.*, 19: 211.

Weber, W.J., J.C. Morris, 1963. *J. Sanit.Eng. Div. Am. Soc. Civ. Eng.*, 89: 31-60.

Yang, X., B. Al-Duri, 2005. *J. Colloid Interf. Sci.*, 287: 25-34.

Yavuz, Ö., Y. Altunkaynak, F. Güzel, 2003. *Water Res.*, 37: 948.